Measurement of Charged Hadron Production in Z-Tagged Jets in Proton-Proton Collisions at $\sqrt{s} = 8$ TeV

R. Aaij *et al.*[*]
(LHCb Collaboration)

(Received 19 April 2019; revised manuscript received 13 June 2019; published 4 December 2019)

The production of charged hadrons within jets recoiling against a Z boson is measured in proton-proton collision data at $\sqrt{s} = 8$ TeV recorded by the LHCb experiment. The charged-hadron structure of the jet is studied longitudinally and transverse to the jet axis for jets with transverse momentum $p_T > 20$ GeV and in the pseudorapidity range $2.5 < \eta < 4$. These are the first measurements of jet hadronization at these forward rapidities and also the first where the jet is produced in association with a Z boson. In contrast to previous hadronization measurements at the Large Hadron Collider, which are dominated by gluon jets, these measurements probe predominantly light-quark jets which are found to be more longitudinally and transversely collimated with respect to the jet axis when compared to the previous gluon dominated measurements. Therefore, these results provide valuable information on differences between quarks and gluons regarding nonperturbative hadronization dynamics.

DOI: 10.1103/PhysRevLett.123.232001

Quantum chromodynamics (QCD), the theory of the strong interaction, is unique amongst the fundamental forces due to the nonperturbative processes that confine quarks and gluons, collectively referred to as partons, within bound-state hadrons. The parton structure of protons has been the focus of intense research efforts; however, the understanding of how hadrons arise from scattered partons is limited in comparison. Perturbative QCD calculations utilize fragmentation functions to determine cross sections of hadron production from scattered partons. Fragmentation functions describe the probability for a particular parton to transform into a particular hadron [1–3]. Several global fits to experimental data have provided parametrized fragmentation functions (see, e.g., Ref. [4] and references therein). However, there is a significant lack of understanding in the mechanisms through which hadrons are formed in the nonperturbative hadronization process and therefore additional data are required.

Fragmentation function studies have been performed using inclusive hadron production at e^+e^- colliders, which benefit from a simpler environment free of initial-state gluon radiation [5–13]. Semi-inclusive deep-inelastic-scattering measurements have also been used to constrain fragmentation functions at smaller values of Q^2, the momentum transfer [14,15]. Additionally, inclusive hadron production measurements have been used to study fragmentation functions in the more complex environment, relative to interactions involving leptons, of proton-proton (pp) collisions [16–18]. However, such measurements are limited by the lack of an explicit way to relate the scattered parton to the final-state hadron. Measuring fragmentation functions with respect to high transverse momentum (p_T) jets offers a unique opportunity to study hadron production relative to an object that is correlated to the scattered parton. For example, the transverse profile, in addition to the longitudinal dynamics of hadrons within jets, can be used to study fragmentation functions in the longitudinal and transverse directions with respect to the jet axis. Such multidimensional measurements that go beyond inclusive hadrons, or those that consider correlations between particles, have the potential to answer unique questions within QCD related to universality, factorization, and the importance of color-charge flow [19,20].

This Letter reports a study of charged hadrons produced in jets recoiling against a Z boson, also referred to as Z-tagged jets, in the forward region of pp collisions (throughout this Letter the notation Z includes both the Z^0 and virtual γ^* contributions). The longitudinal momentum fraction, z, the momentum transverse to the jet axis, j_T, and the radial distribution, r, of charged hadrons are measured with respect to the jet axis in the laboratory frame, defined as

$$z \equiv \frac{\mathbf{p}_{\text{jet}} \cdot \mathbf{p}_{\text{hadron}}}{|\mathbf{p}_{\text{jet}}|^2}, \tag{1}$$

$$j_T \equiv \frac{|\mathbf{p}_{\text{jet}} \times \mathbf{p}_{\text{hadron}}|}{|\mathbf{p}_{\text{jet}}|}, \tag{2}$$

[*]Full author list given at the end of the article.

and

$$r \equiv \sqrt{(\phi_{\text{jet}} - \phi_{\text{hadron}})^2 + (y_{\text{jet}} - y_{\text{hadron}})^2}. \quad (3)$$

Here, $\mathbf{p}$ is the three-momentum vector, ϕ is the azimuthal angle, and y is the rapidity. The data sample is selected from an integrated luminosity of approximately 2 fb^{-1} collected at a center-of-mass energy $\sqrt{s} = 8$ TeV with the LHCb detector in 2012. Events with only one reconstructed primary vertex are analyzed to better identify signatures of a hard two-to-two partonic scattering. Jets are clustered with the anti-k_T algorithm [21] using a distance parameter $R = 0.5$ and are measured differentially in p_T for $p_T > 20$ GeV, and in the pseudorapidity range $2.5 < \eta < 4$. (In this Letter, natural units ($c = \hbar = 1$) are used.) Charged hadrons within the jet are required to have $p_T > 0.25$ GeV, momentum $p > 4$ GeV, and to lie within the jet cone such that $\Delta R < 0.5$, where $\Delta R \equiv \sqrt{(\phi_{\text{jet}} - \phi_{\text{hadron}})^2 + (\eta_{\text{jet}} - \eta_{\text{hadron}})^2}$. The distributions are unfolded to account for the detector response and to facilitate comparisons with theoretical and numerical predictions. This is the first measurement of charged hadrons within jets produced in association with a Z boson, as well as the first measurement of charged hadrons in jets at these forward pseudorapidities. The $Z +$ jet process is primarily sensitive to light quark jets, as demonstrated by PYTHIA in this kinematic range [22,23]. Thus, these data provide new and complementary information to previous jet substructure measurements in the inclusive jet channel at midrapidity in hadronic collisions, which are sensitive to primarily gluon jets [24–29]. Recent results at midrapidity in the isolated photon-jet channel can also probe fragmentation differences when a photon, rather than a massive vector boson, is measured opposite the jet [30].

The LHCb detector is a single-arm forward spectrometer covering the pseudorapidity range $2 < \eta < 5$, described in detail in Refs. [31,32]. Simulations are used to evaluate the detector performance with regard to the jet reconstruction, track-in-jet reconstruction, and to validate the analysis methods. The simulated $pp \to Z + \text{jet} + X$ events are generated using PYTHIA8 [23] with a specific LHCb configuration [33]. Decays of hadronic particles are described by EVTGEN [34], and final-state radiation in the simulation is generated using PHOTOS [35]. Finally, the GEANT4 toolkit [36] is used to simulate the interactions of the particles with the detector, as described in Ref. [37].

This analysis uses the same data set as that used for the $Z +$ jet cross section measurement, where events are selected and Z bosons are measured via their dimuon decay as described in Ref. [38]. Candidate events are required to pass a trigger [39], which selects muons with $p_T > 10$ GeV. Only events that contain two high-p_T muons are retained. The muons are required to satisfy track-reconstruction and muon-identification criteria, as in Refs. [38,40], and are also required to fall within the fiducial region of $2 < \eta < 4.5$, where the detector performance is well understood. Finally, the dimuon system must have an invariant mass, $M_{\mu\mu}$, within the range $60 < M_{\mu\mu} < 120$ GeV.

Jet reconstruction is performed using a particle flow algorithm [41], where the charged and neutral particles are clustered using the anti-k_T algorithm as implemented in Ref. [42]. Reconstructed jets with $p_T > 15$ GeV that lie within $2.5 < \eta < 4$ are analyzed. The $15 < p_T < 20$ GeV region is included to avoid inefficiencies at the lower p_T limit of the measurement in the unfolding procedure. The pseudorapidity requirement ensures that the full jet cone lies within the fiducial area of the LHCb detector. Selection requirements are placed on the jets to reduce the rate of jets not associated with the partonic process producing the Z boson, which is already suppressed by the requirement of a single reconstructed primary vertex in the event. Additionally, the decay muons from the Z boson must not be contained within the jet cone. Only jets that are on the azimuthal away-side of the Z boson, defined by $\Delta\phi_{Z-\text{jet}} \equiv |\phi_Z - \phi_{\text{jet}}| > 7\pi/8$, are analyzed. The jet energy calibrations are the same as those used in Ref. [38]. Charged hadrons within the jet are identified by the particle flow algorithm utilizing the particle-identification systems and several track-quality criteria [32]. The charged hadrons must also satisfy $\Delta R < 0.5$, which ensures that the corresponding tracks fall within the tracking acceptance.

The methods used to determine the charged-hadron fragmentation distributions are as described in Refs. [24,27,43]. The fragmentation distributions are corrected for tracking inefficiencies and two-dimensionally unfolded for resolution effects, which primarily occur due to the jet energy resolution. The unfolded fragmentation distributions are then normalized by the total number of $Z +$ jet events in a given jet p_T bin, which is determined separately from the hadron-in-jet unfolding procedure. A test of the method described here and below, performed with the reconstructed simulation samples, confirmed that the generated distributions were reproduced for all observables studied, within the statistical uncertainties of the simulated sample. In this analysis, the Z -boson p_T is integrated to provide the statistical precision to measure the fragmentation as a function of jet p_T. The integral of the fragmentation distributions then corresponds to the mean multiplicity of charged hadrons within the jet.

The number of $Z +$ jet pairs in each jet p_T bin is corrected to account for reconstruction and selection inefficiencies, and is determined independently from and normalizes the fragmentation distributions. The muon detection efficiencies are determined in data using the technique employed in the inclusive weak boson cross section measurements of LHCb [40,44]. The jet reconstruction efficiency is evaluated from simulation, and is greater than 90% for jets with $p_T > 20$ GeV. A correction is also applied to account for differences

between the number of events produced and measured in a given p_T bin due to the jet p_T resolution. This correction is determined from simulation, and is less than 10%. The method described above is cross checked by comparing the results to a full Bayesian unfolding [45] as implemented in Ref. [46]. The two methods agree to within 1%.

Simulation is used to determine the tracking efficiency and to account for effects from misreconstructed tracks that are incorrectly measured inside or outside of the jet cone. The efficiency is evaluated as a function of momentum and pseudorapidity and applied on a per-track basis. The efficiency decreases for $p > 150$ GeV due to a requirement on the uncertainty of the track bending radius which is part of the particle flow algorithm and has a larger effect at high momentum. The efficiencies were found to be independent of the observables z, j_T and r in the simulated sample. To validate the efficiency corrections procedure, the simulation sample is split in half and the efficiencies are determined with one half and applied to the other. Good recovery of the generated charged hadron distributions in p and η is observed. Within the statistical precision of the sample the tracking efficiency does not depend on the jet p_T.

The effects of bin migration in jet p_T and in the fragmentation observables on the fragmentation distributions, primarily due to the jet energy and momentum resolutions, are corrected using the two-dimensional Bayesian unfolding method. Response matrices are constructed for each fragmentation observable using simulated samples that study the correlations between the generated and reconstructed yields in bins of $[z, p_T^{\text{jet}}]$, $[j_T, p_T^{\text{jet}}]$, and $[r, p_T^{\text{jet}}]$. Typically the bin migration is less than 5%; however, it can be larger for more extreme values of the fragmentation variables, for example at large z. The number of iterations in the Bayesian unfolding procedure is selected to be the minimum number for which the relative change in the fragmentation functions at $z \approx 0.05$ is smaller than 0.2% per additional iteration in all of the jet p_T bins. Based on this criterion, the unfolding is iterated seven times for each observable.

Systematic uncertainties that arise from the uncertainties on the various efficiencies are assigned to the number of $Z +$ jet pairs measured in each jet p_T bin. The uncertainty in the muon reconstruction efficiency is negligible. Systematic uncertainties on the jet reconstruction are evaluated as in Ref. [38] by comparing the jet reconstruction quality requirements in simulation and data. Similarly to the muon efficiencies, the precision with which the uncertainty of the jet reconstruction corrections are determined, due to the limited simulation sample size, is also evaluated; however, this is found to be negligible compared to the jet reconstruction quality requirement uncertainty of 1.9%. The normalization is not corrected for $Z +$ jet background events, and thus a systematic uncertainty of 1.7% is assigned for the impurity of both Z bosons and jets in the measurement, as determined in Refs. [38,40]. Effects from pile up are also studied and found to be negligible. The total normalization uncertainty of 2.7% is determined by adding these components in quadrature.

The jet-energy scale and resolution are also considered as sources of systematic uncertainty. The jet-energy scale and its uncertainty have been studied in previous measurements of the $Z +$ jet cross section [38,41]. To estimate these effects, the scale is varied by one standard deviation of its uncertainty. New unfolding matrices are constructed with this modification, and the difference in the fragmentation distributions determined with the modified and nominal response matrices is taken as a systematic uncertainty. Similarly, the systematic uncertainty due to the jet-energy resolution is evaluated by smearing each component of the jet momentum by an additional term corresponding to the uncertainty on the jet resolution and constructing new response matrices. The difference between the nominal and smeared unfolded charged hadron-in-jet distributions is taken as the systematic uncertainty on the jet-energy resolution.

The unfolding method is validated with two different tests. The first test is performed by splitting the simulated sample in two and using one half to generate the response matrices with which the other half is unfolded. Recovery of the generator-level fragmentation distributions is observed and average deviations from perfect agreement are 2%, which is assigned as an uncertainty related to the unfolding procedure. A second test is performed by splitting the simulated sample in half by Z -boson p_T, and performing a similar test to the previous one to check for any uncertainty associated with the assumed prior. The results again deviate from perfect agreement by about 2%, confirming that a 2% systematic uncertainty on the unfolding procedure is appropriate.

The track selection requirements, tracking efficiency, and charged-hadron identification are also studied as sources of systematic uncertainty. The track selection uncertainty is assigned by requiring a tight fake-track removal criterion and repeating the analysis. The differences in the final fragmentation distributions with and without this requirement are taken as systematic uncertainties. The track selection uncertainty is typically less than 5%; however, it reaches a maximum of approximately 8% at some values of z, j_T, and r in the highest jet p_T bin studied. The systematic uncertainty on the tracking efficiency is determined by smoothing the two-dimensional efficiency and repeating the analysis, which accounts for the statistical precision with which the efficiency is determined. The resulting distributions are compared to the nominal distributions and the differences are taken as uncertainties on the tracking efficiency; these are generally less than 3% but rise up to 10% in some bins. Uncertainties associated to misidentifying charged hadrons are also considered by comparing the nominal fragmentation

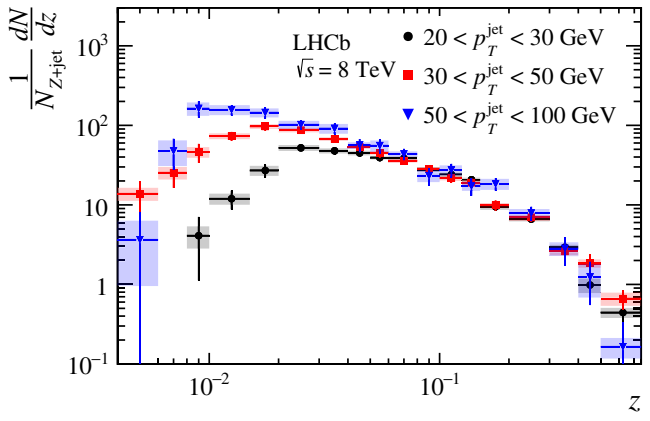

FIG. 1. Distributions of the longitudinal momentum fraction of the hadron with respect to the jet in three bins of jet p_T. The bars (boxes) show the statistical (systematic) uncertainties.

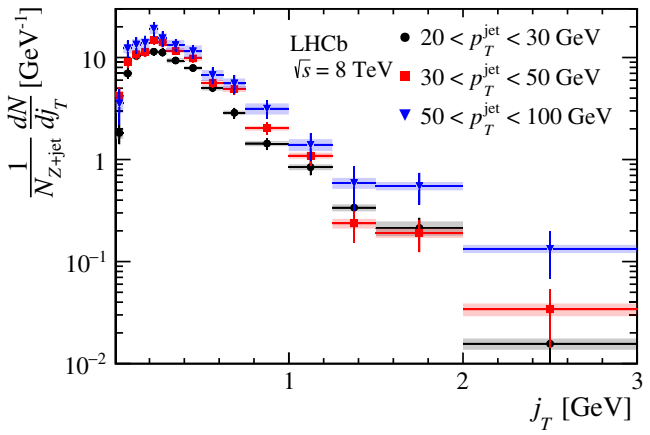

FIG. 2. Distributions of the transverse momentum of charged hadrons with respect to the jet axis in three bins of jet p_T. The bars (boxes) show the statistical (systematic) uncertainties.

functions to those obtained when hadron-to-lepton (and vice versa) misidentification probabilities are considered. These uncertainties are less than 5%, except at large z where the charged pion-to-electron misidentification probability becomes larger [32].

Figure 1 shows the distributions of z in three jet p_T bins. These illustrate that the longitudinal momentum fraction is approximately constant as a function of jet p_T at high z. At low z the fragmentation functions differ, which is a kinematic effect due to the requirement that the track momentum be greater than 4 GeV; therefore, higher p_T jets can probe smaller z. This also reflects that the charged hadron multiplicity increases with jet p_T. Comparing these forward measurements to inclusive jet measurements at central rapidity from ATLAS [24] indicates that the fragmentation functions are not as steeply falling at high z [47]. This may reflect differences between light-quark and gluon fragmentation.

Figures 2 and 3 show the j_T and r distributions of charged hadrons within jets. The j_T profiles show a rounded peak at small j_T which transitions to a perturbative tail at larger j_T as also seen in Ref. [48]. This is indicative of an observable that can be treated in the so-called transverse-momentum-dependent framework [1–3,49], where sensitivity to both a large and small transverse momentum scale is necessary. The radial profiles show that the number of charged hadrons at small r is highly dependent on jet p_T; however, the values are relatively constant as a function of jet p_T at nearly all other values of r. Interestingly, the j_T fragmentation distributions are similar to the central pseudorapidity inclusive jet results; however, these measurements are more collimated in r than the inclusive jet measurements [47]. This behavior in r is correlated to the flatter fragmentation in z and may be a reflection of the different pseudorapidity region or differences in light-quark and gluon fragmentation. We note that the comparisons to the measurements by ATLAS should be qualitative in nature, rather than quantitative, due to the slightly different kinematic criteria placed on each of the measurements. The distributions in j_T and r offer the opportunity to study the interplay between perturbative parton shower and nonperturbative hadronization dynamics. For example, the steeply falling tail of the j_T distributions results from a combination of perturbative radiation and nonperturbative hadronization processes.

The fragmentation functions are compared to predictions from PYTHIA8 $Z+$jet events, where the details of the PYTHIA8 configuration can be found in Ref. [47]. These comparisons are made since the specific LHCb tune contains realistic experimental conditions [33] and also shows that the unfolding procedure is not simply correcting the measured distributions to the predictions from PYTHIA8. An example of the comparison as a function of z is shown in Fig. 4; all of the comparisons described in this text can be found in Ref. [47]. In general, PYTHIA8 underestimates the number of charged hadrons at high z; PYTHIA8 also underestimates the number of charged hadrons at small r.

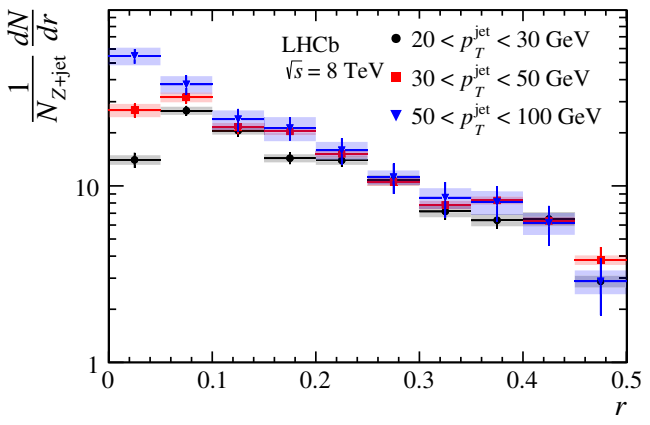

FIG. 3. Radial profile distributions of hadrons with respect to the jet axis in three bins of jet p_T. The bars (boxes) show the statistical (systematic) uncertainties.

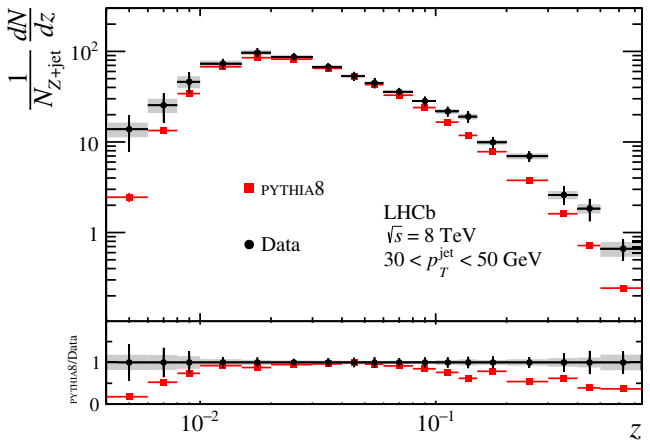

FIG. 4. The z distribution for jets with $30 < p_T < 50$ GeV compared to PYTHIA8 simulation predictions. The bars (boxes) show the statistical (systematic) uncertainties.

Comparisons of the data to predictions from PYTHIA8 as a function of j_T show a consistent shape, but in general PYTHIA underestimates the number of charged hadrons in each bin by approximately 20%. The integral of the ratio of the PYTHIA8 predictions to the data is always less than unity, which is a reflection of the underestimation of the mean charged hadron multiplicity in PYTHIA8.

In summary, the production of charged hadrons in jets recoiling against a Z boson is measured in $\sqrt{s} = 8$ TeV pp collisions by the LHCb experiment. The jets are measured in the fiducial region of $20 < p_T < 100$ GeV and $2.5 < \eta < 4$, while the hadrons are required to have $p_T > 0.25$ GeV, $p > 4$ GeV, and to be located within the jet cone of distance parameter $R = 0.5$. The longitudinal momentum fraction, momentum transverse to the jet axis, and radial profile of the charged hadrons are measured with respect to the jet axis. These results provide insight into hadronization mechanisms as they probe a new kinematic regime. They additionally probe a high fraction of light-quark jets versus gluon jets when compared to midrapidity inclusive jet measurements in the same jet p_T range. The results are compared to predictions from the PYTHIA8 event generator with a specific LHCb configuration, and show that the simulation underestimates the number of high momentum hadrons. Additionally, comparisons with inclusive midrapidity gluon-dominated jet measurements indicate that light quark-dominated jets recoiling against a Z boson at forward rapidity are more collimated in both z and r [47]. This work lays the foundation for a broader hadronization research program at LHCb, utilizing the excellent tracking, particle identification, and heavy-flavor jet tagging capabilities already demonstrated by the LHCb detector [32,50].

We express our gratitude to our colleagues in the CERN accelerator departments for the excellent performance of the LHC. We thank the technical and administrative staff at the LHCb institutes. We acknowledge support from CERN and from the national agencies: CAPES, CNPq, FAPERJ, and FINEP (Brazil); MOST and NSFC (China); CNRS/IN2P3 (France); BMBF, DFG, and MPG (Germany); INFN (Italy); NWO (Netherlands); MNiSW and NCN (Poland); MEN/IFA (Romania); MSHE (Russia); MinECo (Spain); SNSF and SER (Switzerland); NASU (Ukraine); STFC (United Kingdom); NSF (USA). We acknowledge the computing resources that are provided by CERN, IN2P3 (France), KIT and DESY (Germany), INFN (Italy), SURF (Netherlands), PIC (Spain), GridPP (United Kingdom), RRCKI and Yandex LLC (Russia), CSCS (Switzerland), IFIN-HH (Romania), CBPF (Brazil), PL-GRID (Poland), and OSC (USA). We are indebted to the communities behind the multiple open-source software packages on which we depend. Individual groups or members have received support from AvH Foundation (Germany); EPLANET, Marie Skłodowska-Curie Actions, and ERC (European Union); ANR, Labex P2IO and OCEVU, and Région Auvergne-Rhône-Alpes (France); Key Research Program of Frontier Sciences of CAS, CAS PIFI, and the Thousand Talents Program (China); RFBR, RSF, and Yandex LLC (Russia); GVA, XuntaGal, and GENCAT (Spain); the Royal Society and the Leverhulme Trust (United Kingdom); Laboratory Directed Research and Development program of LANL (USA).

[1] J. C. Collins and D. E. Soper, Back-to-back jets in QCD, Nucl. Phys. **B193**, 381 (1981); Erratum, Nucl. Phys. **B213**, 545 (1983).
[2] J. C. Collins and D. E. Soper, Parton distribution and decay functions, Nucl. Phys. **B194**, 445 (1982).
[3] J. Collins, *Foundations of Perturbative QCD*, Cambridge Monographs on Particle Physics, Nuclear Physics and Cosmology Vol. 32 (Cambridge University Press, Cambridge, England, 2011), ISBN 9781107645257.
[4] A. Metz and A. Vossen, Parton fragmentation functions, Prog. Part. Nucl. Phys. **91**, 136 (2016).
[5] D. Buskulic *et al.* (ALEPH Collaboration), Inclusive $\pi^{\pm}$, $K^{\pm}$ and $(p, \bar{p})$ differential cross-sections at the Z resonance, Z. Phys. C **66**, 355 (1995).
[6] R. Akers *et al.* (OPAL Collaboration), Measurement of the production rates of charged hadrons in e^+e^- annihilation at the Z^0, Z. Phys. C **63**, 181 (1994).
[7] R. Akers *et al.* (OPAL Collaboration), A model independent measurement of quark and gluon jet properties and differences, Z. Phys. C **68**, 179 (1995).
[8] P. Abreu *et al.* (DELPHI Collaboration), $\pi^{\pm}$, $K^{\pm}$, p and $\bar{p}$ production in $Z^0 \to q\bar{q}$, $Z^0 \to b\bar{b}$, $Z^0 \to u\bar{u}$, $d\bar{d}$, $s\bar{s}$, Eur. Phys. J. C **5**, 585 (1998).
[9] K. Abe *et al.* (SLD Collaboration), Production of π^+, K^+, K^0, K^{*0}, ϕ, p and Λ^0 in hadronic Z^0 decays, Phys. Rev. D **59**, 052001 (1999).
[10] P. Abreu *et al.* (DELPHI Collaboration), Measurement of the gluon fragmentation function and a comparison of the scaling violation in gluon and quark jets, Eur. Phys. J. C **13**, 573 (2000).

[11] J. P. Lees *et al.* (*BABAR* Collaboration), Production of charged pions, kaons, and protons in e^+e^- annihilations into hadrons at $\sqrt{s} = 10.54$ GeV, Phys. Rev. D **88**, 032011 (2013).

[12] M. Leitgab *et al.* (Belle Collaboration), Precision Measurement of Charged Pion and Kaon Differential Cross Sections in e^+e^- Annihilation at $\sqrt{s} = 10.52$ GeV, Phys. Rev. Lett. **111**, 062002 (2013).

[13] R. Seidl *et al.* (Belle Collaboration), Transverse momentum dependent production cross sections of charged pions, kaons and protons produced in inclusive e^+e^- annihilation at $\sqrt{s} = 10.58$ GeV, Phys. Rev. D **99**, 112006 (2019).

[14] A. Airapetian *et al.* (HERMES Collaboration), Multiplicities of charged pions and kaons from semi-inclusive deep-inelastic scattering by the proton and the deuteron, Phys. Rev. D **87**, 074029 (2013).

[15] M. Aghasyan *et al.* (COMPASS Collaboration), Transverse-momentum-dependent multiplicities of charged hadrons in muon-deuteron deep inelastic scattering, Phys. Rev. D **97**, 032006 (2018).

[16] J. Adams *et al.* (STAR Collaboration), Identified hadron spectra at large transverse momentum in p + p and d + Au collisions at $\sqrt{s_{\mathrm{NN}}} = 200$ GeV, Phys. Lett. B **637**, 161 (2006).

[17] I. Arsene *et al.* (BRAHMS Collaboration), Production of Mesons and Baryons at High Rapidity and High p_T in Proton-Proton Collisions at $\sqrt{s} = 200$ GeV, Phys. Rev. Lett. **98**, 252001 (2007).

[18] A. Adare *et al.* (PHENIX Collaboration), Charged-pion cross sections and double-helicity asymmetries in polarized p + p collisions at $\sqrt{s} = 200$ GeV, Phys. Rev. D **91**, 032001 (2015).

[19] J. C. Collins, Leading-twist single-transverse-spin asymmetries: Drell-Yan and deep-inelastic scattering, Phys. Lett. B **536**, 43 (2002).

[20] T. C. Rogers and P. J. Mulders, No generalized transverse momentum dependent factorization in the hadroproduction of high transverse momentum hadrons, Phys. Rev. D **81**, 094006 (2010).

[21] M. Cacciari, G. P. Salam, and G. Soyez, The anti-k_t jet clustering algorithm, J. High Energy Phys. 04 (2008) 063.

[22] T. Sjöstrand, S. Mrenna, and P. Skands, PYTHIA 6.4 physics and manual, J. High Energy Phys. 05 (2006) 026.

[23] T. Sjöstrand, S. Mrenna, and P. Skands, A brief introduction to PYTHIA 8.1, Comput. Phys. Commun. **178**, 852 (2008).

[24] G. Aad *et al.* (ATLAS Collaboration), Measurement of the jet fragmentation function and transverse profile in proton-proton collisions at a center-of-mass energy of 7 TeV with the ATLAS detector, Eur. Phys. J. C **71**, 1795 (2011).

[25] S. Chatrchyan *et al.* (CMS Collaboration), Measurement of jet fragmentation in PbPb and pp collisions at $\sqrt{s_{\mathrm{NN}}} = 2.76$ TeV, Phys. Rev. C **90**, 024908 (2014).

[26] B. Abelev *et al.* (ALICE Collaboration), Charged jet cross sections and properties in proton-proton collisions at $\sqrt{s} = 7$ TeV, Phys. Rev. D **91**, 112012 (2015).

[27] M. Aaboud *et al.* (ATLAS Collaboration), Measurement of jet fragmentation in 5.02 TeV proton-lead and proton-proton collisions with the ATLAS detector, Nucl. Phys. **A978**, 65 (2018).

[28] M. Aaboud *et al.* (ATLAS Collaboration), Measurement of the Soft-Drop Jet Mass in pp Collisions at $\sqrt{s} = 13$ TeV with the ATLAS Detector, Phys. Rev. Lett. **121**, 092001 (2018).

[29] S. Acharya *et al.* (ALICE Collaboration), Charged jet cross section and fragmentation in proton-proton collisions at $\sqrt{s} = 7$ TeV, Phys. Rev. D **99**, 012016 (2019).

[30] M. Aaboud *et al.* (ATLAS Collaboration), Comparison of Fragmentation Functions for Jets Dominated by Light Quarks and Gluons from pp and Pb + Pb Collisions in ATLAS, Phys. Rev. Lett. **123**, 042001 (2019).

[31] A. A. Alves, Jr. *et al.* (LHCb Collaboration), The LHCb detector at the LHC, J. Instrum. **3**, S08005 (2008).

[32] R. Aaij *et al.* (LHCb Collaboration), LHCb detector performance, Int. J. Mod. Phys. A **30**, 1530022 (2015).

[33] I. Belyaev *et al.*, Handling of the generation of primary events in Gauss, the LHCb simulation framework, J. Phys. Conf. Ser. **331**, 032047 (2011).

[34] D. J. Lange, The EvtGen particle decay simulation package, Nucl. Instrum. Methods A **462**, 152 (2001).

[35] P. Golonka and Z. Was, PHOTOS Monte Carlo: A precision tool for QED corrections in Z and W decays, Eur. Phys. J. C **45**, 97 (2006).

[36] S. Agostinelli *et al.* (GEANT4 Collaboration), GEANT4: A simulation toolkit, Nucl. Instrum. Methods **A506**, 250 (2003); J. Allison *et al.* (GEANT4 Collaboration), GEANT4 developments and applications, IEEE Trans. Nucl. Sci. **53**, 270 (2006).

[37] M. Clemencic, G. Corti, S. Easo, C. R. Jones, S. Miglioranzi, M. Pappagallo, and P. Robbe, The LHCb simulation application, Gauss: Design, evolution and experience, J. Phys. Conf. Ser. **331**, 032023 (2011).

[38] R. Aaij *et al.* (LHCb Collaboration), Measurement of forward W and Z boson production in association with jets in proton-proton collisions at $\sqrt{s} = 8$ TeV, J. High Energy Phys. 05 (2016) 131.

[39] R. Aaij *et al.*, The LHCb trigger and its performance in 2011, J. Instrum. **8**, P04022 (2013).

[40] R. Aaij *et al.* (LHCb Collaboration), Measurement of forward W and Z boson production in pp collisions at $\sqrt{s} = 8$ TeV, J. High Energy Phys. 01 (2016) 155.

[41] R. Aaij *et al.* (LHCb Collaboration), Study of forward Z + jet production in pp collisions at $\sqrt{s} = 7$ TeV, J. High Energy Phys. 01 (2014) 033.

[42] M. Cacciari, G. P. Salam, and G. Soyez, FastJet user manual, Eur. Phys. J. C **72**, 1896 (2012).

[43] R. Aaij *et al.* (LHCb Collaboration), Study of J/ψ Production in Jets, Phys. Rev. Lett. **118**, 192001 (2017).

[44] R. Aaij *et al.* (LHCb Collaboration), Measurement of the forward Z boson cross-section in pp collisions at $\sqrt{s} = 7$ TeV, J. High Energy Phys. 08 (2015) 039.

[45] G. D'Agostini, A multidimensional unfolding method based on Bayes' theorem, Nucl. Instrum. Methods A **362**, 487 (1995).

[46] T. Adye, Unfolding algorithms and tests using RooUnfold, arXiv:1105.1160.

[47] See Supplemental Material at http://link.aps.org/supplemental/10.1103/PhysRevLett.123.232001 for further details.

[48] S. Acharya *et al.* (ALICE Collaboration), Jet fragmentation transverse momentum measurements from di-hadron correlations in $\sqrt{s} = 7$ TeV pp and $\sqrt{s_{\mathrm{NN}}} = 5.02$ TeV p-Pb collisions, J. High Energy Phys. 03 (2019) 169.

[49] J. C. Collins, D. E. Soper, and G. F. Sterman, Transverse momentum distribution in Drell-Yan pair and W and Z boson production, Nucl. Phys. **B250**, 199 (1985).

[50] R. Aaij *et al.* (LHCb Collaboration), Identification of beauty and charm quark jets at LHCb, J. Instrum. **10**, P06013 (2015).

R. Aaij,[29] C. Abellán Beteta,[46] B. Adeva,[43] M. Adinolfi,[50] C. A. Aidala,[77] Z. Ajaltouni,[7] S. Akar,[61] P. Albicocco,[20] J. Albrecht,[12] F. Alessio,[44] M. Alexander,[55] A. Alfonso Albero,[42] G. Alkhazov,[35] P. Alvarez Cartelle,[57] A. A. Alves Jr.,[43] S. Amato,[2] Y. Amhis,[9] L. An,[19] L. Anderlini,[19] G. Andreassi,[45] M. Andreotti,[18] J. E. Andrews,[62] F. Archilli,[29] J. Arnau Romeu,[8] A. Artamonov,[41] M. Artuso,[63] K. Arzymatov,[39] E. Aslanides,[8] M. Atzeni,[46] B. Audurier,[24] S. Bachmann,[14] J. J. Back,[52] S. Baker,[57] V. Balagura,[9,b] W. Baldini,[18,44] A. Baranov,[39] R. J. Barlow,[58] S. Barsuk,[9] W. Barter,[57] M. Bartolini,[21] F. Baryshnikov,[73] V. Batozskaya,[33] B. Batsukh,[63] A. Battig,[12] V. Battista,[45] A. Bay,[45] F. Bedeschi,[26] I. Bediaga,[1] A. Beiter,[63] L. J. Bel,[29] S. Belin,[24] N. Beliy,[4] V. Bellee,[45] N. Belloli,[22,c] K. Belous,[41] I. Belyaev,[36] G. Bencivenni,[20] E. Ben-Haim,[10] S. Benson,[29] S. Beranek,[11] A. Berezhnoy,[37] R. Bernet,[46] D. Berninghoff,[14] E. Bertholet,[10] A. Bertolin,[25] C. Betancourt,[46] F. Betti,[17,d] M. O. Bettler,[51] Ia. Bezshyiko,[46] S. Bhasin,[50] J. Bhom,[31] M. S. Bieker,[12] S. Bifani,[49] P. Billoir,[10] A. Birnkraut,[12] A. Bizzeti,[19,e] M. Bjørn,[59] M. P. Blago,[44] T. Blake,[52] F. Blanc,[45] S. Blusk,[63] D. Bobulska,[55] V. Bocci,[28] O. Boente Garcia,[43] T. Boettcher,[60] A. Bondar,[40,f] N. Bondar,[35] S. Borghi,[58,44] M. Borisyak,[39] M. Borsato,[14] M. Boubdir,[11] T. J. V. Bowcock,[56] C. Bozzi,[18,44] S. Braun,[14] M. Brodski,[44] J. Brodzicka,[31] A. Brossa Gonzalo,[52] D. Brundu,[24,44] E. Buchanan,[50] A. Buonaura,[46] C. Burr,[58] A. Bursche,[24] J. S. Butter,[29] J. Buytaert,[44] W. Byczynski,[44] S. Cadeddu,[24] H. Cai,[67] R. Calabrese,[18,g] S. Cali,[20] R. Calladine,[49] M. Calvi,[22,c] M. Calvo Gomez,[42,h] A. Camboni,[42,h] P. Campana,[20] D. H. Campora Perez,[44] L. Capriotti,[17,d] A. Carbone,[17,d] G. Carboni,[27] R. Cardinale,[21] A. Cardini,[24] P. Carniti,[22,c] K. Carvalho Akiba,[2] G. Casse,[56] M. Cattaneo,[44] G. Cavallero,[21] R. Cenci,[26,i] M. G. Chapman,[50] M. Charles,[10,44] Ph. Charpentier,[44] G. Chatzikonstantinidis,[49] M. Chefdeville,[6] V. Chekalina,[39] C. Chen,[3] S. Chen,[24] S.-G. Chitic,[44] V. Chobanova,[43] M. Chrzaszcz,[44] A. Chubykin,[35] P. Ciambrone,[20] X. Cid Vidal,[43] G. Ciezarek,[44] F. Cindolo,[17] P. E. L. Clarke,[54] M. Clemencic,[44] H. V. Cliff,[51] J. Closier,[44] V. Coco,[44] J. A. B. Coelho,[9] J. Cogan,[8] E. Cogneras,[7] L. Cojocariu,[34] P. Collins,[44] T. Colombo,[44] A. Comerma-Montells,[14] A. Contu,[24] G. Coombs,[44] S. Coquereau,[42] G. Corti,[44] C. M. Costa Sobral,[52] B. Couturier,[44] G. A. Cowan,[54] D. C. Craik,[60] A. Crocombe,[52] M. Cruz Torres,[1] R. Currie,[54] C. L. Da Silva,[78] E. Dall'Occo,[29] J. Dalseno,[43,j] C. D'Ambrosio,[44] A. Danilina,[36] P. d'Argent,[14] A. Davis,[58] O. De Aguiar Francisco,[44] K. De Bruyn,[44] S. De Capua,[58] M. De Cian,[45] J. M. De Miranda,[1] L. De Paula,[2] M. De Serio,[16,k] P. De Simone,[20] J. A. de Vries,[29] C. T. Dean,[55] W. Dean,[77] D. Decamp,[6] L. Del Buono,[10] B. Delaney,[51] H.-P. Dembinski,[13] M. Demmer,[12] A. Dendek,[32] D. Derkach,[74] O. Deschamps,[7] F. Desse,[9] F. Dettori,[24] B. Dey,[68] A. Di Canto,[44] P. Di Nezza,[20] S. Didenko,[73] H. Dijkstra,[44] F. Dordei,[24] M. Dorigo,[26,l] A. C. dos Reis,[1] A. Dosil Suárez,[43] L. Douglas,[55] A. Dovbnya,[47] K. Dreimanis,[56] L. Dufour,[44] G. Dujany,[10] P. Durante,[44] J. M. Durham,[78] D. Dutta,[58] R. Dzhelyadin,[41,a] M. Dziewiecki,[14] A. Dziurda,[31] A. Dzyuba,[35] S. Easo,[53] U. Egede,[57] V. Egorychev,[36] S. Eidelman,[40,f] S. Eisenhardt,[54] U. Eitschberger,[12] R. Ekelhof,[12] L. Eklund,[55] S. Ely,[63] A. Ene,[34] S. Escher,[11] S. Esen,[29] T. Evans,[61] A. Falabella,[17] C. Färber,[44] N. Farley,[49] S. Farry,[56] D. Fazzini,[22,c] M. Féo,[44] P. Fernandez Declara,[44] A. Fernandez Prieto,[43] F. Ferrari,[17,d] L. Ferreira Lopes,[45] F. Ferreira Rodrigues,[2] S. Ferreres Sole,[29] M. Ferro-Luzzi,[44] S. Filippov,[38] R. A. Fini,[16] M. Fiorini,[18,g] M. Firlej,[32] C. Fitzpatrick,[44] T. Fiutowski,[32] F. Fleuret,[9,b] M. Fontana,[44] F. Fontanelli,[21,m] R. Forty,[44] V. Franco Lima,[56] M. Frank,[44] C. Frei,[44] J. Fu,[23,n] W. Funk,[44] E. Gabriel,[54] A. Gallas Torreira,[43] D. Galli,[17,d] S. Gallorini,[25] S. Gambetta,[54] Y. Gan,[3] M. Gandelman,[2] P. Gandini,[23] Y. Gao,[3] L. M. Garcia Martin,[76] J. García Pardiñas,[46] B. Garcia Plana,[43] J. Garra Tico,[51] L. Garrido,[42] D. Gascon,[42] C. Gaspar,[44] G. Gazzoni,[7] D. Gerick,[14] E. Gersabeck,[58] M. Gersabeck,[58] T. Gershon,[52] D. Gerstel,[8] Ph. Ghez,[6] V. Gibson,[51] O. G. Girard,[45] P. Gironella Gironell,[42] L. Giubega,[34] K. Gizdov,[54] V. V. Gligorov,[10] C. Göbel,[65] D. Golubkov,[36] A. Golutvin,[57,73] A. Gomes,[1,o] I. V. Gorelov,[37] C. Gotti,[22,c] E. Govorkova,[29] J. P. Grabowski,[14] R. Graciani Diaz,[42] L. A. Granado Cardoso,[44] E. Graugés,[42] E. Graverini,[46] G. Graziani,[19] A. Grecu,[34] R. Greim,[29] P. Griffith,[24] L. Grillo,[58] L. Gruber,[44] B. R. Gruberg Cazon,[59] C. Gu,[3] E. Gushchin,[38] A. Guth,[11] Yu. Guz,[41,44] T. Gys,[44] T. Hadavizadeh,[59] C. Hadjivasiliou,[7] G. Haefeli,[45] C. Haen,[44] S. C. Haines,[51] B. Hamilton,[62] Q. Han,[68] X. Han,[14] T. H. Hancock,[59] S. Hansmann-Menzemer,[14] N. Harnew,[59] T. Harrison,[56] C. Hasse,[44] M. Hatch,[44] J. He,[4] M. Hecker,[57] K. Heinicke,[12] A. Heister,[12] K. Hennessy,[56] L. Henry,[76] M. Heß,[70] J. Heuel,[11] A. Hicheur,[64] R. Hidalgo Charman,[58] D. Hill,[59] M. Hilton,[58] P. H. Hopchev,[45] J. Hu,[14] W. Hu,[68] W. Huang,[4] Z. C. Huard,[61]

W. Hulsbergen,[29] T. Humair,[57] M. Hushchyn,[74] D. Hutchcroft,[56] D. Hynds,[29] P. Ibis,[12] M. Idzik,[32] P. Ilten,[49] A. Inglessi,[35] A. Inyakin,[41] K. Ivshin,[35] R. Jacobsson,[44] S. Jakobsen,[44] J. Jalocha,[59] E. Jans,[29] B. K. Jashal,[76] A. Jawahery,[62] F. Jiang,[3] M. John,[59] D. Johnson,[44] C. R. Jones,[51] C. Joram,[44] B. Jost,[44] N. Jurik,[59] S. Kandybei,[47] M. Karacson,[44] J. M. Kariuki,[50] S. Karodia,[55] N. Kazeev,[74] M. Kecke,[14] F. Keizer,[51] M. Kelsey,[63] M. Kenzie,[51] T. Ketel,[30] B. Khanji,[44] A. Kharisova,[75] C. Khurewathanakul,[45] K. E. Kim,[63] T. Kirn,[11] V. S. Kirsebom,[45] S. Klaver,[20] K. Klimaszewski,[33] S. Koliiev,[48] M. Kolpin,[14] R. Kopecna,[14] P. Koppenburg,[29] I. Kostiuk,[29,48] O. Kot,[48] S. Kotriakhova,[35] M. Kozeiha,[7] L. Kravchuk,[38] M. Kreps,[52] F. Kress,[57] S. Kretzschmar,[11] P. Krokovny,[40,f] W. Krupa,[32] W. Krzemien,[33] W. Kucewicz,[31,p] M. Kucharczyk,[31] V. Kudryavtsev,[40,f] G. J. Kunde,[78] A. K. Kuonen,[45] T. Kvaratskheliya,[36] D. Lacarrere,[44] G. Lafferty,[58] A. Lai,[24] D. Lancierini,[46] G. Lanfranchi,[20] C. Langenbruch,[11] T. Latham,[52] C. Lazzeroni,[49] R. Le Gac,[8] R. Lefèvre,[7] A. Leflat,[37] F. Lemaitre,[44] O. Leroy,[8] T. Lesiak,[31] B. Leverington,[14] H. Li,[66] P.-R. Li,[4,q] X. Li,[78] Y. Li,[5] Z. Li,[63] X. Liang,[63] T. Likhomanenko,[72] R. Lindner,[44] F. Lionetto,[46] V. Lisovskyi,[9] G. Liu,[66] X. Liu,[3] D. Loh,[52] A. Loi,[24] I. Longstaff,[55] J. H. Lopes,[2] G. Loustau,[46] G. H. Lovell,[51] D. Lucchesi,[25,r] M. Lucio Martinez,[43] Y. Luo,[3] A. Lupato,[25] E. Luppi,[18,g] O. Lupton,[52] A. Lusiani,[26] X. Lyu,[4] F. Machefert,[9] F. Maciuc,[34] V. Macko,[45] P. Mackowiak,[12] S. Maddrell-Mander,[50] O. Maev,[35,44] K. Maguire,[58] D. Maisuzenko,[35] M. W. Majewski,[32] S. Malde,[59] B. Malecki,[44] A. Malinin,[72] T. Maltsev,[40,f] H. Malygina,[14] G. Manca,[24,s] G. Mancinelli,[8] D. Marangotto,[23,n] J. Maratas,[7,t] J. F. Marchand,[6] U. Marconi,[17] C. Marin Benito,[9] M. Marinangeli,[45] P. Marino,[45] J. Marks,[14] P. J. Marshall,[56] G. Martellotti,[28] M. Martinelli,[44,22] D. Martinez Santos,[43] F. Martinez Vidal,[76] A. Massafferri,[1] M. Materok,[11] R. Matev,[44] A. Mathad,[46] Z. Mathe,[44] V. Matiunin,[36] C. Matteuzzi,[22] K. R. Mattioli,[77] A. Mauri,[46] E. Maurice,[9,b] B. Maurin,[45] M. McCann,[57,44] A. McNab,[58] R. McNulty,[15] J. V. Mead,[56] B. Meadows,[61] C. Meaux,[8] N. Meinert,[70] D. Melnychuk,[33] M. Merk,[29] A. Merli,[23,n] E. Michielin,[25] D. A. Milanes,[69] E. Millard,[52] M.-N. Minard,[6] L. Minzoni,[18,g] D. S. Mitzel,[14] A. Mödden,[12] A. Mogini,[10] R. D. Moise,[57] T. Mombächer,[12] I. A. Monroy,[69] S. Monteil,[7] M. Morandin,[25] G. Morello,[20] M. J. Morello,[26,u] J. Moron,[32] A. B. Morris,[8] R. Mountain,[63] H. Mu,[3] F. Muheim,[54] M. Mukherjee,[68] M. Mulder,[29] D. Müller,[44] J. Müller,[12] K. Müller,[46] V. Müller,[12] C. H. Murphy,[59] D. Murray,[58] P. Naik,[50] T. Nakada,[45] R. Nandakumar,[53] A. Nandi,[59] T. Nanut,[45] I. Nasteva,[2] M. Needham,[54] N. Neri,[23,n] S. Neubert,[14] N. Neufeld,[44] R. Newcombe,[57] T. D. Nguyen,[45] C. Nguyen-Mau,[45,v] S. Nieswand,[11] R. Niet,[12] N. Nikitin,[37] N. S. Nolte,[44] A. Oblakowska-Mucha,[32] V. Obraztsov,[41] S. Ogilvy,[55] D. P. O'Hanlon,[17] R. Oldeman,[24,s] C. J. G. Onderwater,[71] J. D. Osborn,[77] A. Ossowska,[31] J. M. Otalora Goicochea,[2] T. Ovsiannikova,[36] P. Owen,[46] A. Oyanguren,[76] P. R. Pais,[45] T. Pajero,[26,u] A. Palano,[16] M. Palutan,[20] G. Panshin,[75] A. Papanestis,[53] M. Pappagallo,[54] L. L. Pappalardo,[18,g] W. Parker,[62] C. Parkes,[58,44] G. Passaleva,[19,44] A. Pastore,[16] M. Patel,[57] C. Patrignani,[17,d] A. Pearce,[44] A. Pellegrino,[29] G. Penso,[28] M. Pepe Altarelli,[44] S. Perazzini,[17] D. Pereima,[36] P. Perret,[7] L. Pescatore,[45] K. Petridis,[50] A. Petrolini,[21,m] A. Petrov,[72] S. Petrucci,[54] M. Petruzzo,[23,n] B. Pietrzyk,[6] G. Pietrzyk,[45] M. Pikies,[31] M. Pili,[59] D. Pinci,[28] J. Pinzino,[44] F. Pisani,[44] A. Piucci,[14] V. Placinta,[34] S. Playfer,[54] J. Plews,[49] M. Plo Casasus,[43] F. Polci,[10] M. Poli Lener,[20] M. Poliakova,[63] A. Poluektov,[8] N. Polukhina,[73,w] I. Polyakov,[63] E. Polycarpo,[2] G. J. Pomery,[50] S. Ponce,[44] A. Popov,[41] D. Popov,[49,13] S. Poslavskii,[41] E. Price,[50] C. Prouve,[43] V. Pugatch,[48] A. Puig Navarro,[46] H. Pullen,[59] G. Punzi,[26,i] W. Qian,[4] J. Qin,[4] R. Quagliani,[10] B. Quintana,[7] N. V. Raab,[15] B. Rachwal,[32] J. H. Rademacker,[50] M. Rama,[26] M. Ramos Pernas,[43] M. S. Rangel,[2] F. Ratnikov,[39,74] G. Raven,[30] M. Ravonel Salzgeber,[44] M. Reboud,[6] F. Redi,[45] S. Reichert,[12] F. Reiss,[10] C. Remon Alepuz,[76] Z. Ren,[3] V. Renaudin,[59] S. Ricciardi,[53] S. Richards,[50] K. Rinnert,[56] P. Robbe,[9] A. Robert,[10] A. B. Rodrigues,[45] E. Rodrigues,[61] J. A. Rodriguez Lopez,[69] M. Roehrken,[44] S. Roiser,[44] A. Rollings,[59] V. Romanovskiy,[41] A. Romero Vidal,[43] J. D. Roth,[77] M. Rotondo,[20] M. S. Rudolph,[63] T. Ruf,[44] J. Ruiz Vidal,[76] J. J. Saborido Silva,[43] N. Sagidova,[35] B. Saitta,[24,s] V. Salustino Guimaraes,[65] C. Sanchez Gras,[29] C. Sanchez Mayordomo,[76] B. Sanmartin Sedes,[43] R. Santacesaria,[28] C. Santamarina Rios,[43] M. Santimaria,[20,44] E. Santovetti,[27,x] G. Sarpis,[58] A. Sarti,[20,y] C. Satriano,[28,z] A. Satta,[27] M. Saur,[4] D. Savrina,[36,37] S. Schael,[11] M. Schellenberg,[12] M. Schiller,[55] H. Schindler,[44] M. Schmelling,[13] T. Schmelzer,[12] B. Schmidt,[44] O. Schneider,[45] A. Schopper,[44] H. F. Schreiner,[61] M. Schubiger,[45] S. Schulte,[45] M. H. Schune,[9] R. Schwemmer,[44] B. Sciascia,[20] A. Sciubba,[28,y] A. Semennikov,[36] E. S. Sepulveda,[10] A. Sergi,[49,44] N. Serra,[46] J. Serrano,[8] L. Sestini,[25] A. Seuthe,[12] P. Seyfert,[44] M. Shapkin,[41] T. Shears,[56] L. Shekhtman,[40,f] V. Shevchenko,[72] E. Shmanin,[73] B. G. Siddi,[18] R. Silva Coutinho,[46] L. Silva de Oliveira,[2] G. Simi,[25,r] S. Simone,[16,k] I. Skiba,[18] N. Skidmore,[14] T. Skwarnicki,[63] M. W. Slater,[49] J. G. Smeaton,[51] E. Smith,[11] I. T. Smith,[54] M. Smith,[57] M. Soares,[17] l. Soares Lavra,[1] M. D. Sokoloff,[61] F. J. P. Soler,[55] B. Souza De Paula,[2] B. Spaan,[12] E. Spadaro Norella,[23,n] P. Spradlin,[55] F. Stagni,[44] M. Stahl,[14] S. Stahl,[44] P. Stefko,[45] S. Stefkova,[57] O. Steinkamp,[46] S. Stemmle,[14] O. Stenyakin,[41] M. Stepanova,[35] H. Stevens,[12] A. Stocchi,[9]

S. Stone,[63] S. Stracka,[26] M. E. Stramaglia,[45] M. Straticiuc,[34] U. Straumann,[46] S. Strokov,[75] J. Sun,[3] L. Sun,[67] Y. Sun,[62] K. Swientek,[32] A. Szabelski,[33] T. Szumlak,[32] M. Szymanski,[4] Z. Tang,[3] T. Tekampe,[12] G. Tellarini,[18] F. Teubert,[44] E. Thomas,[44] M. J. Tilley,[57] V. Tisserand,[7] S. T'Jampens,[6] M. Tobin,[5] S. Tolk,[44] L. Tomassetti,[18,g] D. Tonelli,[26] D. Y. Tou,[10] R. Tourinho Jadallah Aoude,[1] E. Tournefier,[6] M. Traill,[55] M. T. Tran,[45] A. Trisovic,[51] A. Tsaregorodtsev,[8] G. Tuci,[26,44,i] A. Tully,[51] N. Tuning,[29] A. Ukleja,[33] A. Usachov,[9] A. Ustyuzhanin,[39,74] U. Uwer,[14] A. Vagner,[75] V. Vagnoni,[17] A. Valassi,[44] S. Valat,[44] G. Valenti,[17] M. van Beuzekom,[29] H. Van Hecke,[78] E. van Herwijnen,[44] C. B. Van Hulse,[15] J. van Tilburg,[29] M. van Veghel,[29] A. Vasiliev,[41] R. Vazquez Gomez,[44] P. Vazquez Regueiro,[43] C. Vázquez Sierra,[29] S. Vecchi,[18] J. J. Velthuis,[50] M. Veltri,[19,aa] A. Venkateswaran,[63] M. Vernet,[7] M. Veronesi,[29] M. Vesterinen,[52] J. V. Viana Barbosa,[44] D. Vieira,[4] M. Vieites Diaz,[43] H. Viemann,[70] X. Vilasis-Cardona,[42,h] A. Vitkovskiy,[29] M. Vitti,[51] V. Volkov,[37] A. Vollhardt,[46] D. Vom Bruch,[10] B. Voneki,[44] A. Vorobyev,[35] V. Vorobyev,[40,f] N. Voropaev,[35] R. Waldi,[70] J. Walsh,[26] J. Wang,[3] J. Wang,[5] M. Wang,[3] Y. Wang,[68] Z. Wang,[46] D. R. Ward,[51] H. M. Wark,[56] N. K. Watson,[49] D. Websdale,[57] A. Weiden,[46] C. Weisser,[60] M. Whitehead,[11] G. Wilkinson,[59] M. Wilkinson,[63] I. Williams,[51] M. Williams,[60] M. R. J. Williams,[58] T. Williams,[49] F. F. Wilson,[53] M. Winn,[9] W. Wislicki,[33] M. Witek,[31] G. Wormser,[9] S. A. Wotton,[51] K. Wyllie,[44] D. Xiao,[68] Y. Xie,[68] H. Xing,[66] A. Xu,[3] L. Xu,[3] M. Xu,[68] Q. Xu,[4] Z. Xu,[6] Z. Xu,[3] Z. Yang,[3] Z. Yang,[62] Y. Yao,[63] L. E. Yeomans,[56] H. Yin,[68] J. Yu,[68,bb] X. Yuan,[63] O. Yushchenko,[41] K. A. Zarebski,[49] M. Zavertyaev,[13,w] M. Zeng,[3] D. Zhang,[68] L. Zhang,[3] S. Zhang,[3] W. C. Zhang,[3,cc] Y. Zhang,[44] A. Zhelezov,[14] Y. Zheng,[4] X. Zhu,[3] V. Zhukov,[11,37] J. B. Zonneveld,[54] and S. Zucchelli[17,d]

(LHCb Collaboration)

[1]*Centro Brasileiro de Pesquisas Físicas (CBPF), Rio de Janeiro, Brazil*
[2]*Universidade Federal do Rio de Janeiro (UFRJ), Rio de Janeiro, Brazil*
[3]*Center for High Energy Physics, Tsinghua University, Beijing, China*
[4]*University of Chinese Academy of Sciences, Beijing, China*
[5]*Institute Of High Energy Physics (ihep), Beijing, China*
[6]*Univ. Grenoble Alpes, Univ. Savoie Mont Blanc, CNRS, IN2P3-LAPP, Annecy, France*
[7]*Université Clermont Auvergne, CNRS/IN2P3, LPC, Clermont-Ferrand, France*
[8]*Aix Marseille Univ, CNRS/IN2P3, CPPM, Marseille, France*
[9]*LAL, Univ. Paris-Sud, CNRS/IN2P3, Université Paris-Saclay, Orsay, France*
[10]*LPNHE, Sorbonne Université, Paris Diderot Sorbonne Paris Cité, CNRS/IN2P3, Paris, France*
[11]*I. Physikalisches Institut, RWTH Aachen University, Aachen, Germany*
[12]*Fakultät Physik, Technische Universität Dortmund, Dortmund, Germany*
[13]*Max-Planck-Institut für Kernphysik (MPIK), Heidelberg, Germany*
[14]*Physikalisches Institut, Ruprecht-Karls-Universität Heidelberg, Heidelberg, Germany*
[15]*School of Physics, University College Dublin, Dublin, Ireland*
[16]*INFN Sezione di Bari, Bari, Italy*
[17]*INFN Sezione di Bologna, Bologna, Italy*
[18]*INFN Sezione di Ferrara, Ferrara, Italy*
[19]*INFN Sezione di Firenze, Firenze, Italy*
[20]*INFN Laboratori Nazionali di Frascati, Frascati, Italy*
[21]*INFN Sezione di Genova, Genova, Italy*
[22]*INFN Sezione di Milano-Bicocca, Milano, Italy*
[23]*INFN Sezione di Milano, Milano, Italy*
[24]*INFN Sezione di Cagliari, Monserrato, Italy*
[25]*INFN Sezione di Padova, Padova, Italy*
[26]*INFN Sezione di Pisa, Pisa, Italy*
[27]*INFN Sezione di Roma Tor Vergata, Roma, Italy*
[28]*INFN Sezione di Roma La Sapienza, Roma, Italy*
[29]*Nikhef National Institute for Subatomic Physics, Amsterdam, Netherlands*
[30]*Nikhef National Institute for Subatomic Physics and VU University Amsterdam, Amsterdam, Netherlands*
[31]*Henryk Niewodniczanski Institute of Nuclear Physics Polish Academy of Sciences, Kraków, Poland*
[32]*AGH—University of Science and Technology, Faculty of Physics and Applied Computer Science, Kraków, Poland*
[33]*National Center for Nuclear Research (NCBJ), Warsaw, Poland*
[34]*Horia Hulubei National Institute of Physics and Nuclear Engineering, Bucharest-Magurele, Romania*
[35]*Petersburg Nuclear Physics Institute NRC Kurchatov Institute (PNPI NRC KI), Gatchina, Russia*
[36]*Institute of Theoretical and Experimental Physics NRC Kurchatov Institute (ITEP NRC KI), Moscow, Russia, Moscow, Russia*

[37]Institute of Nuclear Physics, Moscow State University (SINP MSU), Moscow, Russia
[38]Institute for Nuclear Research of the Russian Academy of Sciences (INR RAS), Moscow, Russia
[39]Yandex School of Data Analysis, Moscow, Russia
[40]Budker Institute of Nuclear Physics (SB RAS), Novosibirsk, Russia
[41]Institute for High Energy Physics NRC Kurchatov Institute (IHEP NRC KI), Protvino, Russia, Protvino, Russia
[42]ICCUB, Universitat de Barcelona, Barcelona, Spain
[43]Instituto Galego de Física de Altas Enerxías (IGFAE), Universidade de Santiago de Compostela, Santiago de Compostela, Spain
[44]European Organization for Nuclear Research (CERN), Geneva, Switzerland
[45]Institute of Physics, Ecole Polytechnique Fédérale de Lausanne (EPFL), Lausanne, Switzerland
[46]Physik-Institut, Universität Zürich, Zürich, Switzerland
[47]NSC Kharkiv Institute of Physics and Technology (NSC KIPT), Kharkiv, Ukraine
[48]Institute for Nuclear Research of the National Academy of Sciences (KINR), Kyiv, Ukraine
[49]University of Birmingham, Birmingham, United Kingdom
[50]H.H. Wills Physics Laboratory, University of Bristol, Bristol, United Kingdom
[51]Cavendish Laboratory, University of Cambridge, Cambridge, United Kingdom
[52]Department of Physics, University of Warwick, Coventry, United Kingdom
[53]STFC Rutherford Appleton Laboratory, Didcot, United Kingdom
[54]School of Physics and Astronomy, University of Edinburgh, Edinburgh, United Kingdom
[55]School of Physics and Astronomy, University of Glasgow, Glasgow, United Kingdom
[56]Oliver Lodge Laboratory, University of Liverpool, Liverpool, United Kingdom
[57]Imperial College London, London, United Kingdom
[58]School of Physics and Astronomy, University of Manchester, Manchester, United Kingdom
[59]Department of Physics, University of Oxford, Oxford, United Kingdom
[60]Massachusetts Institute of Technology, Cambridge, Massachusetts, USA
[61]University of Cincinnati, Cincinnati, Ohio, USA
[62]University of Maryland, College Park, Maryland, USA
[63]Syracuse University, Syracuse, New York, USA
[64]Laboratory of Mathematical and Subatomic Physics, Constantine, Algeria
[associated with Universidade Federal do Rio de Janeiro (UFRJ), Rio de Janeiro, Brazil]
[65]Pontifícia Universidade Católica do Rio de Janeiro (PUC-Rio), Rio de Janeiro, Brazil
[associated with Universidade Federal do Rio de Janeiro (UFRJ), Rio de Janeiro, Brazil]
[66]South China Normal University, Guangzhou, China
(associated with Center for High Energy Physics, Tsinghua University, Beijing, China)
[67]School of Physics and Technology, Wuhan University, Wuhan, China
(associated with Center for High Energy Physics, Tsinghua University, Beijing, China)
[68]Institute of Particle Physics, Central China Normal University, Wuhan, Hubei, China
(associated with Center for High Energy Physics, Tsinghua University, Beijing, China)
[69]Departamento de Fisica, Universidad Nacional de Colombia, Bogota, Colombia
(associated with LPNHE, Sorbonne Université, Paris Diderot Sorbonne Paris Cité, CNRS/IN2P3, Paris, France)
[70]Institut für Physik, Universität Rostock, Rostock, Germany
(associated with Physikalisches Institut, Ruprecht-Karls-Universität Heidelberg, Heidelberg, Germany)
[71]Van Swinderen Institute, University of Groningen, Groningen, Netherlands
(associated with Nikhef National Institute for Subatomic Physics, Amsterdam, Netherlands)
[72]National Research Centre Kurchatov Institute, Moscow, Russia
[associated with Institute of Theoretical and Experimental Physics NRC Kurchatov Institute (ITEP NRC KI), Moscow, Russia, Moscow, Russia]
[73]National University of Science and Technology "MISIS", Moscow, Russia
[associated with Institute of Theoretical and Experimental Physics NRC Kurchatov Institute (ITEP NRC KI), Moscow, Russia, Moscow, Russia]
[74]National Research University Higher School of Economics, Moscow, Russia
(associated with Yandex School of Data Analysis, Moscow, Russia)
[75]National Research Tomsk Polytechnic University, Tomsk, Russia
[associated with Institute of Theoretical and Experimental Physics NRC Kurchatov Institute (ITEP NRC KI), Moscow, Russia, Moscow, Russia]
[76]Instituto de Fisica Corpuscular, Centro Mixto Universidad de Valencia—CSIC, Valencia, Spain
(associated with ICCUB, Universitat de Barcelona, Barcelona, Spain)
[77]University of Michigan, Ann Arbor, USA
(associated with Syracuse University, Syracuse, New York, USA)
[78]Los Alamos National Laboratory (LANL), Los Alamos, USA
(associated with Syracuse University, Syracuse, New York, USA)

[a]Deceased.
[b]Also at Laboratoire Leprince-Ringuet, Palaiseau, France.
[c]Also at Università di Milano Bicocca, Milano, Italy.
[d]Also at Università di Bologna, Bologna, Italy.
[e]Also at Università di Modena e Reggio Emilia, Modena, Italy.
[f]Also at Novosibirsk State University, Novosibirsk, Russia.
[g]Also at Università di Ferrara, Ferrara, Italy.
[h]Also at LIFAELS, La Salle, Universitat Ramon Llull, Barcelona, Spain.
[i]Also at Università di Pisa, Pisa, Italy.
[j]Also at H.H. Wills Physics Laboratory, University of Bristol, Bristol, United Kingdom.
[k]Also at Università di Bari, Bari, Italy.
[l]Also at Sezione INFN di Trieste, Trieste, Italy.
[m]Also at Università di Genova, Genova, Italy.
[n]Also at Università degli Studi di Milano, Milano, Italy.
[o]Also at Universidade Federal do Triângulo Mineiro (UFTM), Uberaba-MG, Brazil.
[p]Also at AGH—University of Science and Technology, Faculty of Computer Science, Electronics and Telecommunications, Kraków, Poland.
[q]Also at Lanzhou University, Lanzhou, China.
[r]Also at Università di Padova, Padova, Italy.
[s]Also at Università di Cagliari, Cagliari, Italy.
[t]Also at MSU—Iligan Institute of Technology (MSU-IIT), Iligan, Philippines.
[u]Also at Scuola Normale Superiore, Pisa, Italy.
[v]Also at Hanoi University of Science, Hanoi, Vietnam.
[w]Also at P.N. Lebedev Physical Institute, Russian Academy of Science (LPI RAS), Moscow, Russia.
[x]Also at Università di Roma Tor Vergata, Roma, Italy.
[y]Also at Università di Roma La Sapienza, Roma, Italy.
[z]Also at Università della Basilicata, Potenza, Italy.
[aa]Also at Università di Urbino, Urbino, Italy.
[bb]Also at Physics and Micro Electronic College, Hunan University, Changsha City, China.
[cc]Also at School of Physics and Information Technology, Shaanxi Normal University (SNNU), Xi'an, China.